

pubs.acs.org/journal/ascecg Research Article

Identifying the Transition from Hydrothermal Carbonization to Liquefaction of Biomass in a Batch System

Giulia Ischia, Hanifrahmawan Sudibyo, Antonio Miotello, Jefferson William Tester, Luca Fiori, and Jillian L. Goldfarb*



Cite This: ACS Sustainable Chem. Eng. 2024, 12, 4539–4550



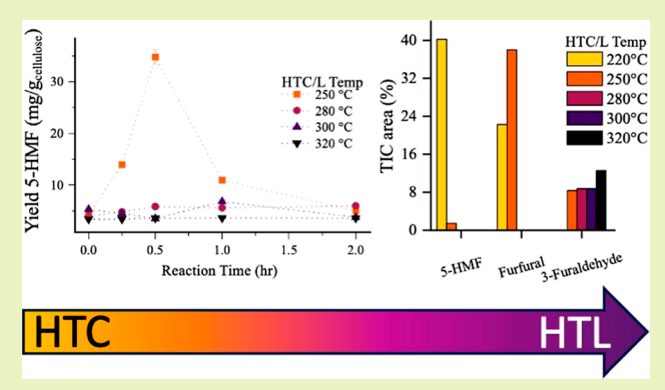
ACCESS I

III Metrics & More

Article Recommendations

s Supporting Information

ABSTRACT: The transition from mild to harsh hydrothermal conditions involves the passage from progressive hydrothermal carbonization (HTC) to liquefaction (HTL) of biomass, shifting products from solid to oily phases. Understanding the reaction pathways biomass undergoes during hydrothermal processing can help researchers tune operating conditions according to the desired products. This work investigates the transition from HTC to HTL of two model and one heterogeneous biomass: cellulose, lignin, and wood chips. The experimental method approaches a "real-time" study by sampling the reaction slurry during hydrothermal operation. Analyses were performed on the solid and liquid (aqueous and oily) products obtained from processing over a range of temperatures (220–320 °C) and residence times (0–2 h).



Hydrochars' thermal stability and carbon content increase with process severity (time and temperature). For all the substrates, thermogravimetric analyses show that volatile, thermally unstable compounds form at moderate temperatures. Samples drawn during the reaction with immediate liquid analysis enabled us to follow the evolution of organics, mainly carboxylic acids, furans, and phenol derivatives, providing an insight into hydrothermal reaction pathways. Overall, as temperature increases, organic acids and furans progressively transform to ketones and phenol-derivatives, while 5-hydroxymethylfurfural yield reaches a maximum at 30 min at 250 and 280 °C.

KEYWORDS: hydrochar, biocrude, hydrothermal process, process severity

1. INTRODUCTION

The impacts of and role of fossil fuels in anthropogenic climate change are well-recognized and wide-reaching. Most carbon-based compounds used to produce chemicals are derived from petroleum, and around 80% of the global energy demand is met by fossil fuels. Hydrothermal processes (HPs) could support a shift from a fossil-based to a zero-carbon economy by converting waste biomass into renewable solid and liquid fuels.

HPs exploit the unique properties of liquid water under high temperature and pressure to decompose biomass into a solid hydrochar, an oily biocrude phase, an aqueous process water containing dissolved organics, and a gas phase comprised predominantly of CO₂.⁴ Hydrothermal processing is well suited to the conversion of wet substrates as the substrate's moisture content serves as the reaction medium. As such, these processes are potential waste management strategies to treat heterogeneous organic wastes, manures, and sludges. Within the hydrothermal processing realm, we commonly think of hydrothermal carbonization (HTC) and liquefaction (HTL) as separate processes. HTC (roughly) occurs at mild conditions (180–250 °C and 10–50 bar) and predominantly converts

biomass into hydrochar, which may find applications as a solid biofuel and feedstock for producing advanced carbon materials. The harsher conditions of HTL (250–370 °C and up to 220 bar) favor the formation of a liquid biocrude, which can be further converted into transportation fuels or platform chemicals. HTL biocrude often has a lower oxygen content and is less viscous than bio-oil produced through other thermochemical processes like pyrolysis. Over the past decade, growing recognition of the potential of HP to valorize wet waste led to the creation of companies like TerraNova, Ingelia, and Carborem for HTC (mainly operating in the waste treatment field) and the first HTL pilot plants. Only 10,11

Significant research exists on both HTC and HTL, spanning process chemistry, influence of operating parameters on product distribution and quality, process, and reactor

Received: November 25, 2023 Revised: February 17, 2024 Accepted: February 21, 2024 Published: March 1, 2024





modeling, and upgrading of products. 6,12 While many reviews provide a holistic view of both HTC and HTL (e.g., 6,13,14), experimental research often focuses on the two HPs separately,¹⁴ This approach can be explained by the inherent complexity of each conversion, their chemical end points, and the different product aims of the two processes. 15,16 Pecchi et al. recently demonstrated the existence of a discontinuity in the enthalpy of reaction that occurs around 250 °C for cellulose, supporting the idea that HTC and HTL are disparate processes at least in a thermodynamic sense. 17 However, the chemical products' transition is not discrete but rather involves a progressive shift from the carbonization to liquefaction of the biomass. As temperature increases, the properties of the reaction environment change due to the variation of thermophysical properties of liquid water-for example, its density and relative dielectric constant decrease (the latter from 78.5 to 20 moving from 20 to 300 °C)—affecting the yields and properties of the products. 18,19 Disparate papers across the literature unravel the main reaction pathways of model biomasses, although the exact reactions are still unclear due to their complexity.²

Hydrothermal reactions are of both a heterogeneous and homogeneous nature, depending on the substrate. Typical reactions include hydrolysis, decomposition, recombination, and aromatization.²¹ Hydrolysis is generally the first step occurring in a low temperature range (below 200 °C) and consists of the partial depolymerization of biomass macromolecules into their monomers. 20,22 For example, carbohydrates hydrolyze to monosaccharides (pentoses and hexoses), lignin to monolignols, lipids to fatty acids and glycerol, and proteins to amino acids.²³ As temperature increases, monosaccharides decompose to alcohols, furanic acids, and short-chain fatty acids; lignin monomers rehydrate into acids, furans, and aldehydes and can further form alcohols and ketones; proteins decompose to amines, short-chain fatty acids, and aldehydes; and fatty acids undergo esterification.²⁰ Dissolved compounds (like HMF or phenol fragments) condense onto the solid phase often, as nano/micro spheres (often referred to as secondary char).⁵ By increasing temperature (above 280-300 °C) into the HTL range, reactive fragments may recombine and other larger molecules (for example, long-chain fatty acids) are dissolved into the liquid phase to form a biocrude. Over the HTL range, the biomass composition is crucial in determining the resulting biocrude properties. For example, the presence of amino acids activates Maillard reactions that inhibit the formation of repolymerized solids and favor biocrude formation.^{20,23} Finally, reaction pathways are affected by parameters like residence time, heating and cooling rates, and pH. For example, longer residence times (particularly at lower temperatures) favor solid phase production while fast heating/cooling rates enhance biocrude yield.²⁰

The heterogeneous nature of biomass limits our ability to understand the reaction pathways that biomass follows from HTC through HTL. Despite this complexity, a general approach to understand the overall reaction pathway can assist with process optimization; tailoring process conditions can maximize the production of target compounds and minimize energy inputs to the process. ²⁴ Data on the products along the hydrothermal spectrum as a function of time are missing from the literature yet are critical components to optimize HP conditions.

Therefore, this work explores the transition from carbonization to liquefaction of two model biomasses (cellulose and lignin) and willow wood chips. Cellulose and lignin are among the building blocks of lignocellulosic feedstocks and are representative of two very different chemistries: cellulose is a carbohydrate composed of glucose units that easily hydrolyze and dissolve into saccharides that further undergo degradation, while lignin is a recalcitrant aromatic heteropolymer whose decomposition produces phenols and methoxy phenols.²⁰ Willow wood (in the form of chips) is used as a representative of lignocellulosic biomass and contains approximately equal proportion of cellulose, lignin and hemicellulose, 25,26 enabling the observation of their combined effects. Data are discussed alongside literature on hemicellulose conversion (commonly represented by xylan)²⁷⁻³⁰ to enrich our understanding of the data presented. The experimental method adopted here approaches a "real-time" study by sampling the reaction slurry during hydrothermal operation over a wide range of operating conditions. Runs were performed in a lab scale batch system and the residence time was measured once the reactor reached the operating temperature (after heating). Therefore, the study does not address the search for optimal process setup nor accounts for the technicalities of the apparatus (e.g., reactor size, continuous/discontinuous operations, or heating time), yet provides insights into the evolution of compounds along the broad hydrothermal spectrum to inform process design.

2. MATERIAL AND METHODS

To trace the chemical pathways from HTC to HTL of biomasses, we examine the solid (hydrochar) and liquid (biocrude and aqueous phases) of reaction HP products across time and temperature.

2.1. Hydrothermal Processing. Hydrothermal runs were performed on microcrystalline cellulose powder (Alfa Aesar, minimum 97% purity), lignin (Sigma-Aldrich low sulfonate content alkali), and willow wood chips sourced from Cornell University in Ithaca, NY. All biomass samples were dried before each run and mixed with distilled water at a fixed biomass-to-water mass ratio of 0.2 to ensure a constant baseline for all experiments. For each hydrothermal run, 30 g of biomass plus water was charged into a Parr Hydrothermal Reactor (stirred, 300 mL, 350 °C, 5000 psi). Before every test, the reactor was flushed three times with pure nitrogen to establish an inert environment. The reactor was stirred at 300 rpm to promote heat and mass transfer and ensure a homogeneous mixture. The reactor was heated to 190, 220, 250, 280, 300, and 320 °C, with each final temperature held for a total residence time of 2 h. To mimic a real-time analysis, during every run, around 4 mL of slurry were sampled at different time intervals of 0, 0.25, 0.5, and 1 h using a dip pipe positioned approximately 1/5 of the height from the bottom of the reactor. The reaction time commenced after the heating time; the reactor heats at approximately 6 °C/min. The hydrochar was separated from the liquid phase using a qualitative filter with a pore size of 2.5 μ m, dried overnight at 105 °C, and then weighed. The solid yield is calculated as the ratio between the mass of hydrochar and the initial biomass mass, based on a dry basis.

2.2. Hydrochar Characterization. Proximate analysis was performed on a TA Instruments Thermogravimetric Analyzer 5500. Between 2 and 8 mg of dry sample were placed into a 70 μ L alumina crucible, heated in high-purity nitrogen at 10 °C/min up to 110 °C and held for 30 min to remove moisture, then at 10 °C/min from 110 to 900 °C and held for 30 min to determine volatile matter (VM). Then, samples were heated from 900 to 950 °C under dry air and held for 30 min, with the loss attributed to fixed oxidizable carbon (FC). Residual mass is referred to as "ash". The extent of sample converted during pyrolysis at any time t, x(t), was computed as

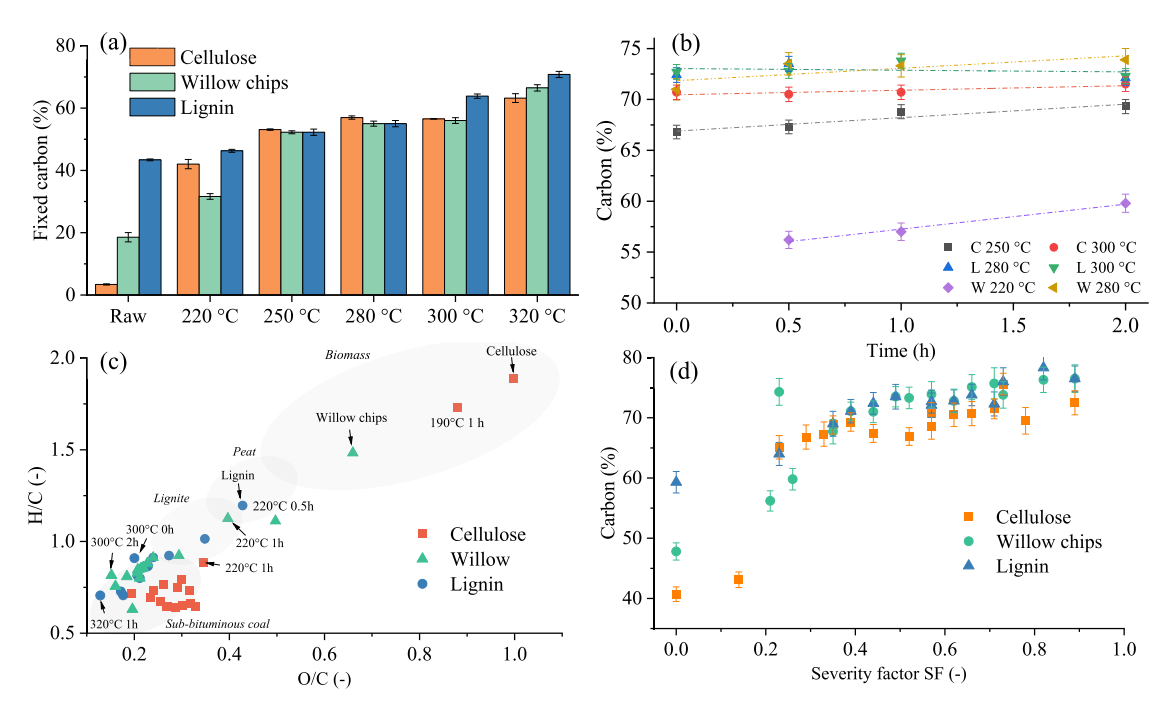


Figure 1. (a) Effect of temperature on fixed carbon content of HCs at 2 h; (b) effect of residence time on carbon content of selected HCs (C = cellulose, L = lignin, W = willow chips); (c) van Krevelen diagram of hydrochars; (d) effect of SF on the carbon content of HCs (0 corresponds to the untreated biomasses). Error bars represent the standard one deviation.

$$x(t) = \frac{m_{\rm dry} - m_t}{m_{\rm dry} - m_{\rm pyr}} \tag{1}$$

where $m_{\rm dry}$ is the dry mass after the sample is held at 110 °C, m_t is the mass at any time t, and $m_{\rm pyr}$ is the residual mass left at the end of the pyrolytic step. Derivative conversion curves (DTG) were constructed by plotting ${\rm d}x/{\rm d}t$ versus temperature.

Ultimate analyses were performed using a CE-440 Elemental Analyzer (Exeter Analytical) to determine carbon (C), hydrogen (H), and nitrogen (N) contents. Oxygen (O) was computed by difference. Tests were performed at least in triplicate. Fourier transform infrared (FTIR) spectra were recorded through a Thermo Fisher FTIR using the KBr pellet technique over a wavenumber range 4000–600 cm⁻¹.

To observe the effects of both temperature and time, the severity factor $(SF)^{5,31}$ was introduced as a function of the residence time (in s) and the reaction temperature T (in K) as

$$SF = 50t^{0.2} \cdot e^{\left(-\frac{3500}{T}\right)} \tag{2}$$

SF has the advantage of providing a "condensed" view of the effects of reaction severity since it accounts simultaneously for the effects of temperature and time, both crucial drivers for hydrothermal conversion. It has limits, like not accounting for the heterogeneous properties of biomass (as it was developed based on cellulose only) and not reflecting HTC mechanisms for various compounds. However, it provides a relative benchmark of the effects of time and temperature used across the literature.

2.3. Characterization of the Liquid Phase. The liquid phase comprises compounds dissolved into the aqueous phase (mainly polar) and a biocrude, conventionally identified as formed by dichloromethane (DCM)-soluble compounds (mainly nonpolar). The separate liquid analyses are intended to provide a wide view of the liquid products' composition, but we note that the distinction between polar and nonpolar compounds is not sharp; compounds may be identified both in the aqueous phase and the biocrude.

The liquid phase was characterized in terms of total organic carbon (TOC), which was measured using an automated Shimdazu TOC-L CSH (with TNM-L unit addition) according to the ASTM D7573 standard. The composition of the aqueous phase was measured using Shimadzu High-Performance Liquid Chromatography (HPLC),

operating with an Ultra Aqueous C18 Column at 30 °C and at a total flow rate of 1.5 mL/min. The mobile phase consists of a 10 mM solution of phosphoric acid and acetonitrile, with a volume ratio of 90/10 for the first 10 min and a ratio of 70/30 from 10 to 50 min of the HPLC program. The detection was performed through a UV—vis detector (SPD-20A) set at a wavelength of 210 nm. HPLC was calibrated using 14 HPLC-grade compounds: glycolic acid (1.256 min), formic acid (1.370 min), lactic acid (1.370 min), propionic acid (1.370 min), levulinic acid (2.470 min), acetic acid (2.741 min), 2(5H) furanone (2.357 min), 5-HMF (3.329 min), furfural (5.418 min), 5-methylfurfural (11.479 min), 1,3 cyclopentanedione (2.575 min), 2-cyclopenten-1-one (4.215 min), phenol (11.980 min), and 2,6 dimethoxyphenol (18.157 min). Then, the sum of the carbon content (in g/L) of all HPLC-detected compounds was referred to as TOC_{HPLC}.

The biocrude was extracted by mixing the hydrothermal liquor with DCM in a 1:1 (by volume) ratio. The dissolved fraction of oil inside the DCM was recovered, and any excess water present in the DCM was removed by mixing it with 0.1 g of anhydrous magnesium sulfate (Fisher Scientific) in a 1.5 mL polypropylene centrifuge tube. Then, the dried biocrude was analyzed via gas chromatography-mass spectroscopy (GC-MS, Shimadzu GC-MS-QP2020 with an AOC-20s auto- sampler). Samples were prepared by diluting 0.5 mL of the dried biocrude with 0.5 mL DCM before injection. The GC-MS oven temperature was set at 40 $^{\circ}$ C, and the sample was injected at 250 $^{\circ}$ C onto a Shimadzu Crossbond 30 m long, 0.25 mm ID column, with a flow of 1 mL/min helium and a split ratio of 15:1. The thermal program of the oven consists of 5 min at 40 °C, ramp at 5 °C/min from 40 to 150 °C, 5 min at 150 °C, ramp at 1.75 °C/min to 250 °C, and 10 min at 250 °C. Interface and ion source temperatures were 250 and 230 °C, respectively. A solvent cut time of 6 min was set on the mass spectrometer, and after 6 min, it was run in scan mode from 15 to 400 m/z using electron ionization. Only peaks with slopes \geq 1500 and durations \geq 2 s were considered, while compounds were identified by spectra through the internal NIST library (match >97%).

3. RESULTS AND DISCUSSION

Biomasses were subjected to hydrothermal treatment at 220, 250, 280, 300, and 320 °C and residence times ranging from 0

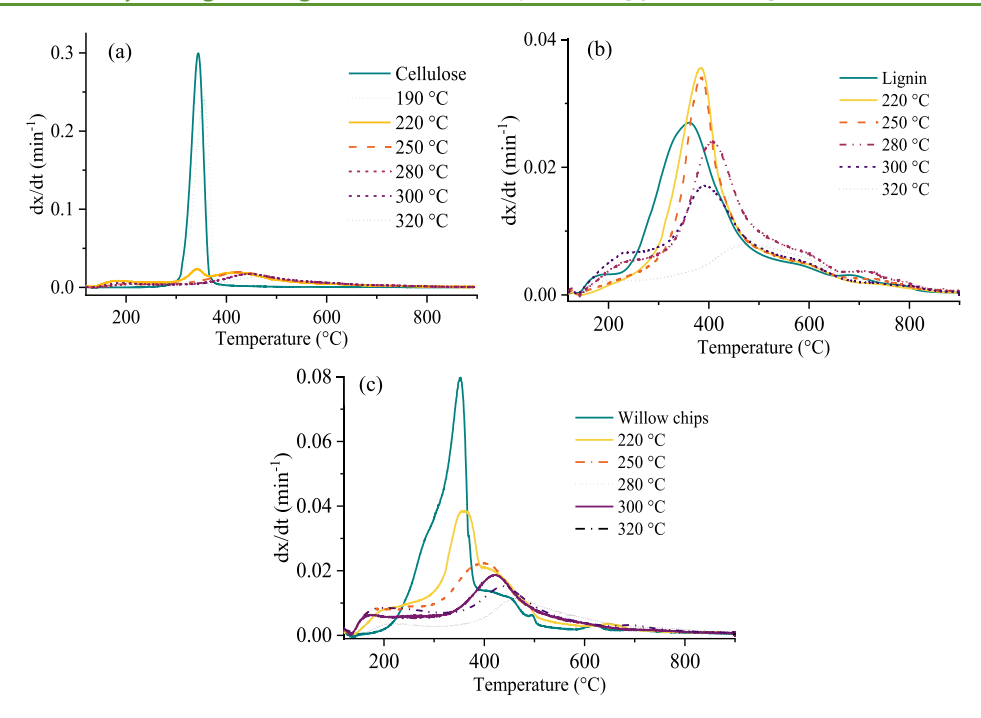


Figure 2. Effect of temperature on DTG curves under pyrolytic conditions (heating rate of 10 °C/min) of hydrochars obtained at 2 h from (a) cellulose, (b) lignin, and (c) willow chips.

to 2 h (zero corresponds to the first moment when the final temperature is reached after the heating phase). Analyses of the hydrochar and the liquid phase drawn during the operation were performed to approach a real-time study and provide as broad and complete a picture as possible of the conversion.

3.1. Evolution of Hydrochar Composition. Biomasses undergo progressive mass loss, VM loss, and aromatization as the process severity, i.e., temperature and time, gets harsher (Figure 1 and Tables S1 and S2, Supporting Information).

The progressive carbonization with severity is well-known in the literature: 5,6,32 severity intensifies gasification and liquefaction reactions, and high temperatures and long residence times favor the decomposition of hydrolyzed organics to CO and CO2, the formation of nonpolar compounds with a low oxygen content (that partition to the oily phase), and aromatization of the solid phase. 15 The van Krevelen diagram (Figure 1c) illustrates how higher temperatures and longer residence times lead to hydrochars that span from the lignite to the sub-bituminous regions. Severity enhances the thermal stability of hydrochars, with DTG curves (Figure 2a-c) showing a progressive shift of the main pyrolytic peak toward higher temperatures and slower reaction rates. Among the feedstocks, lignin reaches the highest level of carbonization in terms of C (78.3%) and FC (70.8%) contents due to its nature as an aromatic heteropolymer. The increase of FC carbon for all the substrates (Figure 1a) highlights how the hydrothermal conversion pushes VM into the liquid phase and enhances the formation of a more stable carbon solid. A high FC can improve the energy potential and energy density of the char, in turn improving the efficiency of heat released during combustion and the reactivity profile. For all the substrates hydrothermally processed above 280 °C, the composition of hydrochars varies slightly with severity due to the predominance of slow bulk reactions in the solid phase and the completion of main liquid reactions. In the HTL region, residence time has a smaller effect on the hydrochar

composition (Figure 1b) than it does over the HTC range, suggesting that the main reactions that decompose the parent feedstock occur during the heating phase and within the HTC region. The slight decrease in solid yields above 280 °C can be attributed more to intensified gasification reactions (favored at higher temperatures) than to an enhanced dissolution process. In this regard, the slow heating rate (6 °C/min) adopted is an impactful process variable as it provides sufficient time for reactions like hydrolysis to go to completion and higher energy-requiring reactions like decarboxylation of the char, as well as char-liquid heterogeneous reactions to occur.

Hydrochars from cellulose do not exhibit significant changes in composition compared to cellulose before 220–250 °C. The "late" start of the cellulose decomposition as compared to other biomasses (especially those containing hemicellulose, sugars, and other less recalcitrant compounds which begin to hydrolyze around 160-170 °C) is known from the literature and is due to the β -(1-4) glycosidic bonds between sugar monomers that confer strong stability to cellulose. ^{30,33} Around 220 °C, solid-liquid reactions (in particular the hydrolysis of β -(1-4) glycosidic bond) start, followed by solid-solid decomposition reactions and ultimately the back polymerization of organics dissolved in the liquid phase onto the solid hydrochar. 30,333 Solid-solid reactions consist of bulk-decomposition reactions, where the bulk part of cellulose undergoes thermal degradation like pyrolysis, forming an aromatic network.³⁴ Intermediate products dissolved in the liquid phase (like 5-HMF deriving from the dehydration of monomers) undergo repolymerization into the solid phase, forming the secondary char.³⁴ Therefore, the HTC range of 220-250 °C shows a coexistence of solid-liquid, solid-solid, and liquid-solid reactions, with residence time highly affecting the final composition (at 250 °C, FC passes from 46.7 to 53.1%, while C passes from 66.8 to 69.3% moving from 0 to 2 h). These data align with the composition ranges generally measured in the HTC literature, which show values of FC in

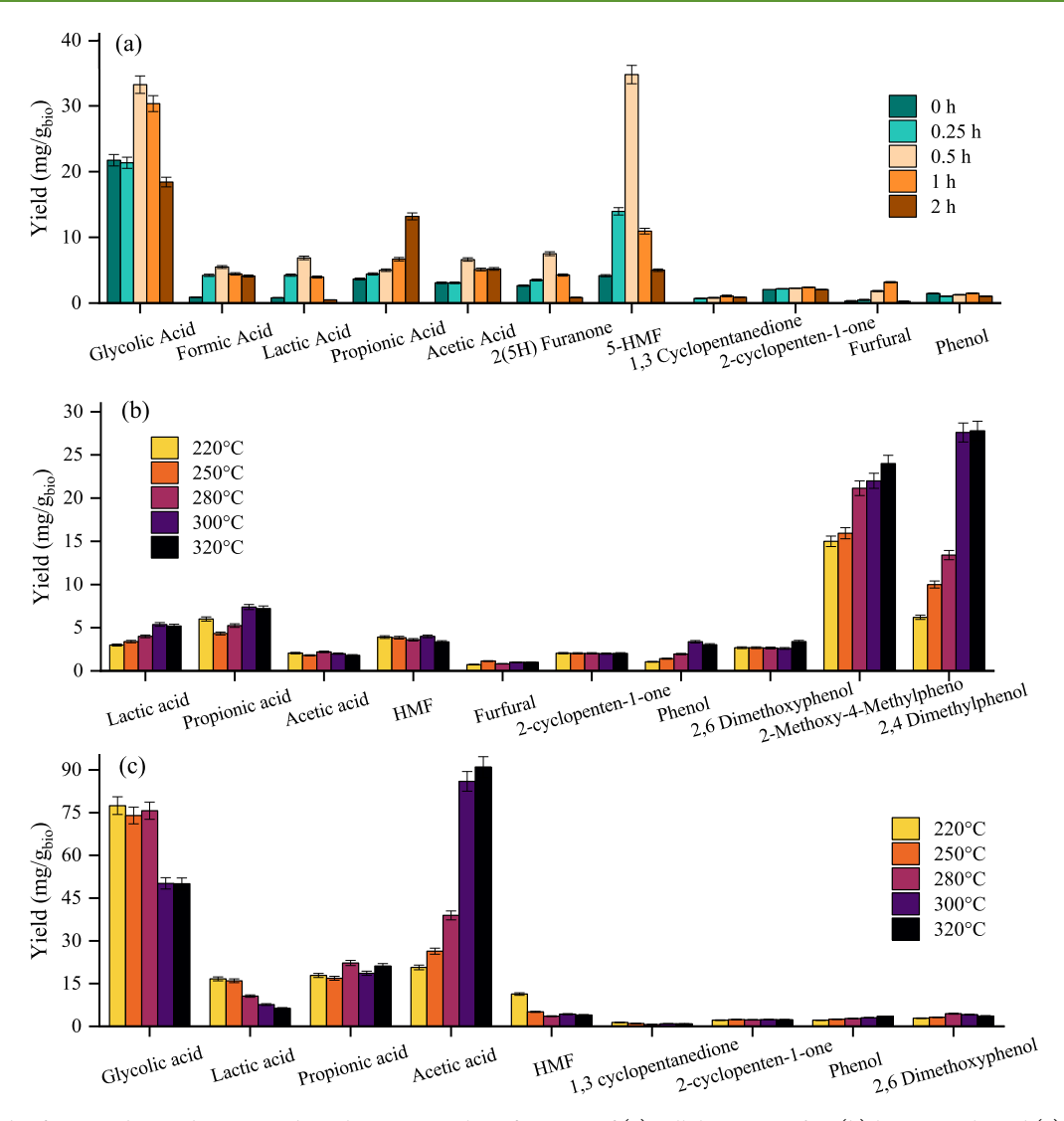


Figure 3. Trends of HPLC-detected compounds in the aqueous phase from HP of (a) cellulose at 250 °C, (b) lignin at 2 h, and (c) willow chips at 2 h. Error bars represent standard deviations.

the range of 42.0-45.7% and C in the range of 71.5-75.5%. 33,35,36 Figure 1b-d provides a condensed view of the effects of severity, showing the passage from a steep to a stable trend moving from low to high SF. Regarding hydrochar thermal profiles (Figure 2a), these can be divided into two/ three stages: the first at 180–220 °C, a second at 345–350 °C due to unreacted cellulose, and a third at 415-465 °C. Since the cellulose main peak is centered at 345 °C, the first and third stages derive from new structures formed during/after HP. The first DTG stage (180-220 °C) is present for all the hydrochars regardless of the HP severity and highlights the presence of thermally unstable species, likely compounds dissolved in the liquor that adsorbed onto the hydrochar surface, as we recently demonstrated in another work.³⁷ The third DTG peak can be attributed to the solid hydrochar itself, as also observed in prior studies.³³ As the SF increases, the third DTG peak position slightly shifts toward higher temperatures and moves from around 415 to 465 °C along the hydrothermal spectrum.

Lignin, like cellulose, undergoes both homogeneous and bulk reactions. Lignin, as an amorphous polymer with a complex aromatic structure and a high initial FC and C content (43.4 and 59.3%, respectively)³⁸ begins to decompose

at low temperatures, yet especially in its nonrefined form, it is never fully decomposed. Its complex aromatic structure is difficult to hydrolyze and requires harsh conditions to break ether bonds (C-O-C) and carbon-carbon bonds (C-C) between the monomers.³⁹ Because of its recalcitrant nature, the hydrochar proximate composition slightly varies between 220, 250, and 280 °C at 0 h (FC 45.9-47.7%); however, this difference is not statistically significant (p > 0.05, two-tailed ttest). Under these conditions, only longer residence times (>1 h) enable significant solid reduction. Solid yields transitioned from 83.4 to 68.1% between 220 and 280 °C (Table S2), accompanied by a concurrent migration of C from the solid to the liquid phase, as discussed later. A harsher decomposition occurs above 300 °C (at 2 h, FC is 63.8 at 300 °C and 70.8 at 320 °C; p < 0.05), and residence time significantly affects the composition. At 320 °C, there is a highly statistically significant enhancement in the C fraction (reaching 78.3 wt %, p < 0.05). As temperature increases, a greater concentration of phenols dissolves into the liquid and repolymerizes back, forming a secondary char phase.³⁹ Like cellulose, lignin DTG profiles (Figure 2b) can be divided into two main stages: an early stage at 180-250 °C, probably due to fragments of partially non converted lignin and thermally unstable compounds deriving

Table 1. TOC Measured, Percentage of TOC Computed from HPLC Data (TOC_{HPLC}), and Percentage of TOC Occupied from Families of Compounds Dissolved into the Aqueous Phase^a

substrate	temp ($^{\circ}$ C)	TOC (g/L)	TOC_{HPLC} (%)	% TOC			
				carboxylic acids	furans and furfurals	ketones	phenol
cellulose	220	31.0	29.7	14.8	12.6	1.7	0.5
	250	15.0	29.5	20.7	4.7	3.1	1.1
	280	14.8	18.8	12.0	2.6	3.0	1.1
	300	11.9	30.8	20.1	4.4	5.0	1.4
	320	12.9	26.2	18.7	3.3	2.7	1.4
lignin	220	12.6	42.6	7.8	4.3	2.4	28.2
	250	21.2	28.6	4.0	2.7	1.4	20.5
	280	21.1	35.5	4.8	2.4	1.4	26.9
	300	21.4	48.7	6.1	2.7	1.4	38.5
	320	30.8	34.6	4.1	1.7	1.0	27.9
willow chips	220	27.4	44.5	35.2	4.7	2.1	2.5
	250	29.4	39.4	33.0	2.0	1.8	2.6
	280	27.9	45.7	39.1	1.5	1.6	3.5
	300	30.3	47.8	41.2	1.6	1.7	3.2
	320	28.0	53.4	46.5	1.6	1.8	3.5

[&]quot;Data refer to different feedstocks and temperatures at a fixed residence time of 2 h. Standard deviations computed from error propagations are always lower than 2.0%.

from the liquid phase, and a second stage at 380-450 °C due to the newly formed carbonized solid phase. The results agree with those from Kang et al., who observed two DTG shoulders for lignin-based hydrochars around 200 °C and 380-410 °C.

Willow chips, composed of approximately 36% cellulose, 25% lignin, and 33% hemicellulose, 25,26 show an intermediate behavior between cellulose and lignin though—as documented throughout the literature 40—certainly not an easily predictable one given reaction synergies between biomass components. Its composition, comprising 47.8% C and 42.0% O, is between that of cellulose (40.1% C, 53.3% O), lignin (59.3% C, 33.8% O), and hemicellulose (for which xylan would have 39.9% C and 53.3% O).²⁷ A temperature of 220 °C already induces carbonization (C increases from 47.8 to 56-60% and FC from 18.5 to 25–30% moving from the raw material to 220 °C), but at a lower degree than cellulose and lignin. This behavior is due to the hemicellulose content, which degrades into sugars at low temperatures due to its random noncrystalline structure and lack of repeating β -(1-4) glycosidic bonds.⁴¹ Previous studies^{42–44} reported that hemicellulose completely or mostly carbonizes even at low temperatures (also 120 °C, with no evidence of unreacted hemicellulose inside hydrochars), indicating that it mostly decomposes in solution into sugar derivatives that partially repolymerize on the hydrochar and form an abundance of hydronium ions, 45 which may explain the enhanced reactivity of the willow chips. Given its tendency for rapid hydrolysis at low temperatures, hemicellulose likely has a minor impact on the hydrochar properties under harsher HP conditions, where cellulose and lignin exert more influence. Above 250 °C, the process severity causes a progressive increase in FC and C content, with a similar elemental and proximate composition of hydrochars from cellulose and lignin. Above 280 °C, solid yields are lower than those of cellulose and lignin-as low as 36.3% at 280 °C Table S2—and the data are comparable with literature conducted on similar substrates.46 The lower solid yield is likely due to the combined decomposition of cellulose and hemicellulose, which increases the acidity of the hydrothermal environment and promotes the accessibility of water molecules to the decomposed material, favoring the migration of C from the

solid to the liquid phase. DTG profiles (Figure 2c) show an intermediate behavior between cellulose and lignin, with a first DTG shoulder at $160-220~^{\circ}\text{C}$ due to poorly thermally stable compounds and a second one at $380-420~^{\circ}\text{C}$ due to the hydrochar itself.

Finally, FTIR spectra were used to observe the variations in functional groups and chemical bonds of hydrochar surfaces. Regarding cellulose (Figure S1), the band at 3600-3000 cm⁻¹ is attributed to the O-H stretching of hydroxylic and carboxylic groups, while at 2920 cm⁻¹ to the vibrations of C–H. The two bands at around 1610 and 1700 $\rm cm^{-1}$ derive from carbohydrates 47,48 and are aldehydes derived from the repolymerization of furanic structures on the hydrochar surface and therefore represent secondary char. The band at 1000-1460 cm⁻¹ in the 250 °C hydrochar is due to the stretching of hydroxylic and O-H. As the severity increases, the intensity of the -OH band decreases due to dehydration reactions, while the decrease of the "furanic" band is due to the progressive consumption of aldehyde groups in cross-linking reactions.⁴⁸ Spectra from the lignin-based hydrochars (Figure S1) show spectra bands due to the stretching vibration of: phenolic and aliphatic -OH groups (3600-2900 cm⁻¹), methyl group C-H (2920 cm⁻¹), phenol and aromatic rings (1595 and 1510 cm⁻¹), bending of guaiacyl groups (1200 cm⁻¹), C–O in primary alcohols (1030 cm⁻¹), and C–H in syringyl (820 cm⁻¹). As temperature increases, the intensity of aliphatic -OH decreases, suggesting the removal of ether groups typical of lignin. Spectra show that the main surface functionality changes occur above 300 °C.

3.2. Evolution of Compounds into the Aqueous Phase and TOC. HPLC data provide insight into the evolution of compounds dissolved in the aqueous phase (Figure 3). Compounds were conventionally divided into four families: carboxylic acids, furans, ketones, and phenols. The distribution among the different families is highly dependent on the substrate. The HP of cellulose leads to carboxylic acids and furans (mainly 5-HMF), lignin to phenol derivatives, and willow chips to a varied composition resembling its poly component nature. Table 1 shows both the TOC of the entire liquid phase (i.e., compounds dissolved into the aqueous phase

and extracted through DCM) and the corresponding fraction of TOC computed from HPLC data. As TOC is a "total" measure, its fluctuations are due to the balance between the release of organics into the liquid phase, repolymerization of dissolved organics, biocrude formations, and a progressive release of carbon in the gas phase (gasification) favored by higher temperatures.⁴ Relevant TOC variations occur, moving from 220 to 250 °C for cellulose and lignin. For cellulose, TOC decreases from 31 to 15 g/L; this is likely due to the repolymerization reactions of dissolved compounds in the liquid to form secondary char. A similar trend was also observed by Becker et al. 50 Regarding lignin, the lowest TOC value at 220 °C (12.6 g/L) is due to its recalcitrant nature. The liquid phase from willow chips does not show significant TOC variation, a trend that agrees with the slow fluctuations in solid yield. Besides, it is worth considering that HPLC does not allow the determination of the entire TOC of the liquid phase (it achieves a maximum identification of around 53.4%). This gap can be attributed to several reasons: difficulty in measuring high molecular weight compounds, the presence of nonpolar compounds (detected instead through GC-MS), carbonaceous nano/microspheres not retained by the filter, and the eventual presence of other colloidal compounds.⁵¹ Further studies could help to clarify the reasons behind the discrepancy.

Regarding the compounds present, carboxylic acids are produced from the degradation of monomers deriving from the hydrolysis of cellulose and hemicellulose, like fructose, galactose, mannose, and xylose (this last is dominant in hemicellulose). Carboxylic acids occupy the highest TOC fraction from willow chips due to the overlapping and interaction between sugars deriving from cellulose and hemicellulose, both present in willow. In the case of lignin, carboxylic acids occupy a small percentage (lower than 7.8%) due to the small/absent presence of sugar derivatives in the feedstock. Among the carboxylic acids, glycolic acid is the dominant compound from cellulose and willow chips. It derives from the oxidation of intermediates (like pyruvaldehyde) produced through the dehydration of fructose derived from the cleavage of carbohydrates from cellulose/hemicellulose.⁵² Glycolic acid decreases with temperature due to its decarboxylation into subproducts. Lactic acid degrades to ethanol through decarboxylation at high temperatures and dehydrates to propionic acid, which slightly increases with temperature. 53 Formic acid derives from the 5-HMF rehydration and is present both in cellulose and lignin, while it is mostly absent in willow chips, where it probably degrades to acetic acid. Similarly, levulinic acid derives from the rehydration of 5-HMF and decreases with temperature since it is consumed by other reactions. For example, it is known that levulinic acid participates in hydrochar formation by embedding itself inside the char as a copolymerized compound. 54 All the feedstocks produce acetic acid, which comes from (1) fructose fragmentation, involving decarboxylation or decarbonylation of lactic acid produced from the oxidation of acetaldehyde derived from glucose and (2) oxidation of HMF and furfurals. 48,55,56 While 5-HMF oxidation plays a minor role compared to fructose fragmentation, its partial oxidation could contribute to its decrease with temperature, together with decarboxylation and decarbonvlation reactions.

Furan and furfural derivatives, mainly consisting of 5-HMF and furfural derived from sugar degradation, were present in the liquid phase of all feedstocks and at the highest

concentrations for cellulose. Even at lower concentrations, they are also present in the aqueous phase from lignin (reaching a maximum of 2.1 mg/ $g_{biomass}$) and result from the rehydration of phenols.²⁰ For cellulose and willow chips (Figure 3a-c), furans and furfurals show a maximum concentration at low processing temperature and have an upward-downward trend over time. Indeed, 5-HMF forms through the direct dehydration of glucose or aldose-ketose isomerization of glucose to fructose with subsequent dehydration. Then, 5-HMF repolymerizes into secondary char and rehydrates into carboxylic acids (mainly formic and levulinic acid).⁵⁷ 5-HMF shows its highest concentration at 220 °C for 1 h, with around 54.1 mg/ g_{bio} for cellulose and 11.3 mg/g_{bio} for willow chips. The lower amount in the liquid phase from willow is due to its variegate composition: hemicellulose, also composed of other pentoses, and lignin contribute to a lower extent than cellulose alone. Figure 3a shows the typical upward-downward trend of 5-HMF over time when it increases up to 1/2 h and then rapidly decreases over time. Furfural results from the dehydration of pentose sugars and the loss of -CH₂O from 5-HMF. 41,58 Under HTL conditions, furfural mostly disappears. Similar behavior was observed in the literature, with no evidence of furfural above 300 °C. 58 In the case of lignin (Figure 3b), the temperature does not show a significant effect on the evolution of these compounds.

Phenolic compounds are the main products of lignin decomposition and occupy around 20.5–38.5% of the TOC of its liquid phase. Lignin itself is characterized by a complex network of three-dimensional and noncrystalline phenolic polymers. All the phenol derivatives' concentrations increase as the temperature increases. This energy input triggers the cleavage of the aromatic structure of lignin, with 2,4-dimethylphenol reaching 27.8 mg/g_{bio} at 320 °C for 2 h. Phenol derives from the hydrolysis of lignin through the cleavage of β -O-4 ether bonds and C–C bonds, while other phenolic compounds derive from demethoxylation and alkylation reactions. Phenol derivatives are present in small quantities in willow chips and cellulose because of the degradation of furfurals and aldehydes/unsaturated intermediates. S9,60

Ketones were detected in smaller amounts, with a predominance of cyclopentanedione and 2-cyclopentenone (C5–C6). Ketones show similar concentrations for all the feedstocks (always less than 5.0% of TOC) and for the different temperatures and times. Ketones are particularly present inside the biocrude, as will be discussed in Section 3.3.

In general, HPLC data could be a starting point for optimizing the recovery of specific chemicals and calibrating kinetic models and scenarios. Among the HPLC-detected compounds, 5-HMF is probably one of the most valuable products since it is a building block to produce biobased chemicals (like dimethylfuran). 5-HMF needs carbohydrate feedstocks and is already produced over the HTC range at mild temperatures and short residence times. Lactic acid and furfurals are other interesting chemicals that are acquiring a rising interest as precursors for biobased products like bioplastic (polylactic acid) and catalysts, respectively. 5

3.3. Evolution of Compounds into the Biocrude. The biocrude phase represents the liquid fraction extracted using DCM and is therefore enriched in nonpolar compounds. GCMS semiquantitative data provide a general overview of the effect of operating conditions on the composition, as reported in Figures 4 and S2.

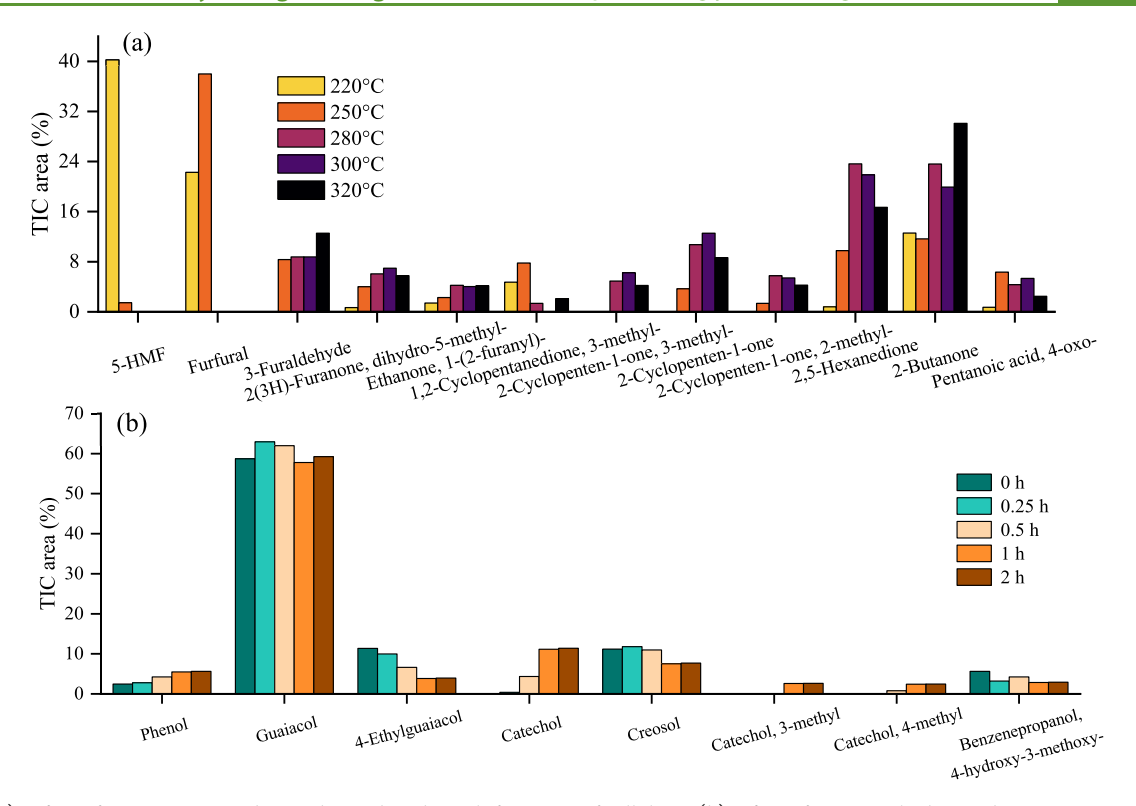


Figure 4. (a) Effect of temperature on biocrude produced at 2 h from HP of cellulose; (b) effect of time on the biocrude composition from HP of lignin at 300 °C. Data are expressed as a percentage of the total chromatogram area (TIC).

As shown in Figure 4a, the biocrude from cellulose mainly consists of furans, ketones, and aldehydes. The total TIC area slightly varies with temperature, indicating that the decomposition of cellulose does not significantly contribute to the formation of biocrude. The literature also shows that biomasses rich in carbohydrates tend to yield less biocrude compared to other biomasses.²⁰ For example, Yang et al. demonstrated a biocrude mass yield of 14.2% for pure cellulose compared to 95.8% for lipids (performing HTL under similar heating rates to our study). 61 The acidic conditions deriving from the large amount of organic acids from sugar hydrolysis promote hydrochar formation, reducing biocrude yield. Adjusting the pH toward alkaline conditions is advantageous for maximizing the conversion of the cellulosic portions of biomass into biocrude. 20,62,63 This adjustment modifies the reaction pathways toward aldol condensation of the light oxygenate products, enhancing the conversion process. In this case, the highest values of TIC area are measured at 220 °C, where the contribution of furans is predominant. Above 220 °C, furans mainly degrade to carboxylic acids that are dissolved in the aqueous phase. At 220 °C, the biocrude is mainly composed of 5-HMF, which then degrades to furfural by losing its acetol group. Then, both 5-HMF and furfural disappear above 250 °C due to their poor solubility inside DCM (they are detected inside the aqueous phase). Above 250 °C, the biocrude consists mainly of ketones (cyclic and linear), whose absolute value remains almost constant as the severity increases (see Supporting Information for data). Cyclic ketones mainly consist of cyclopentanone derivatives in the C5-C6 carbon range (like 2-Cyclopenten-1-one) deriving from the cyclization of fragments deriving from the hydrolysis of carbohydrates.⁶⁴ Linear ketones like 2,5 hexanedione and 2-butanone are also present. A very small fraction of phenols is also produced

(always less than 2.5%) from the dehydration of carbohydrate monomers.

The biocrude from lignin (Figures 4b and S2) mainly comprises oxygenated hydrocarbons (i.e., hydrocarbons that contain oxygenated functional groups), like carbonyl (-C= O) and hydroxyl (-OH) groups. Phenols and phenolic compounds occupy the main fraction of the collected biocrudes. Oxygenated hydrocarbons derive from the hydrolysis and cleavage of the ether bond and C-C bond, which are the most abundant linkages inside lignin.⁵³ As temperature increases, the TIC absolute area increases, indicating a higher biocrude yield, which is also partially balanced by gasification reactions and a progressive repolymerization into secondary char. The majority of compounds are in the range C_6-C_9 , which is typical of gasoline hydrocarbons. 65 Regarding absolute mass yields, the literature reported a biocrude yield of only 3.9% from lignin under a similarly slow heating rate and high solid residue yield, owing to the recalcitrant nature of lignin. Guaiacol (2-Methoxyphenol, $C_7H_8O_2$) is the most abundant detected compound. Its relative area increases up to 300 °C (reaching 59.3%) and then rapidly decreases to 25.1% at 320 °C. Guaiacol derives from the primary depolymerization of coniferyl alcohol, one of the basic monomeric units of lignin. 66 Guaiacol is one of the principal compounds in lignin decomposition and is often used as a model compound to represent it. 66,67 As temperature increases, hydrolysis reactions are favored and provide the H⁺ and OH⁻ necessary for the direct selectivity of guaiacol to form catechol (1,2-Benzenediol, $C_6H_6O_2$). Guaiacol is reactive owing to the weak, easy-tocleave aliphatic bond of the methoxyl group. Catechol then further forms its derivatives, like 3-methylcatechol and 4methylcatechol. Phenol slightly increases up to 320 °C (with the same trend detected through HPLC analysis, Figure 3c), and its relative area ranges between 2.1 and 5.8%. The trend

aligns with the findings of Wahyudiono et al., who observed a consistent increase in the yield of phenol over time, both under subcritical and supercritical conditions, with mass yields achieving 2.5% at 350 °C and 4 h.68 Phenol mainly derives from the direct degradation of guaiacol or the scission of catechol through the formation of phenol radicals.⁶⁶ Then, heavier compounds deriving from the main structure of lignin, like 4-hydroxy-3-methoxy-benzenepropanol, progressively undergo degradation as temperature increases. As shown in Figure 4b, guaiacols form at short residence times, while catechols and phenols increase over time. The trends agree with the mechanism above-mentioned for which guaiacol first forms from lignin monomers and then degrades to catechols. A similar trend was also observed by Forchheim et al.⁶⁹ In general, the composition of the biocrude slightly varies over time, indicating, as with the solid data, that predominant reactions occur during the heating phase.

Willow chips produce a heterogeneous biocrude composed of furans, ketones, and phenols (Figure S2). The total TIC area slightly increases with temperature, in particular from 300 to 320 °C. 5-HMF and furfural occupy the highest fractions over the HTC range (20.7 and 25%, respectively) and derive from both the cellulosic and hemicellulosic fractions. Hemicellulose contributes to the release of pentose and hexose (derived from monomers like xylose, mannose, and glucose, known to be maximized at more mild HTC conditions⁷⁰) which then dehydrate to 5-HMF and furfural. Phenols mainly derive from the lignin fraction, are highly present already at 220 °C, and mainly consist of guaiacol, phenol, and 2,6 dimethoxyphenol. Wang et al. demonstrated that the impact of hemicellulose on both biocrude yield and composition does not change across the investigated hydrothermal range due to its rapid hydrolysis, even at temperatures as low as 120 °C.27 Therefore, the predominant variations in biocrude from willow chips likely primarily arise from the hydrothermal behaviors of its cellulose and lignin fractions and the overall synergy of the hydrothermal environment.

Summarizing, the biocrude consists mainly of cyclopentene derivatives in the cases of cellulose and willow chips (carbohydrate-based feedstocks), while phenol derivatives are the majority of biocrude compounds in the case of lignin. It is worth noting the inherent limitations of characterizing biocrude using GC-MS analysis. For example, the TIC fraction offers insights into the relative composition but not an absolute quantification of constituents, and only a portion of biocrude components is detected, excluding those with greater molecular weights that do not elute from the GC column. Furthermore, the slow heating rates here (around 6 °C/min) enhance the hydrochar formation at the expense of the biocrude. In terms of chemical recovery, the high presence of guaiacol from lignin and willow chips, an important platform chemical used in several fields like the manufacturing of plastics, rubbers, pharmaceuticals, and flavorings, is a promising result.⁷

- **3.4. Overview of Transitions Observed.** By combining the data from the different analyzed phases, we summarize the following considerations regarding the transition from HTC to HTL observed.
 - (1) Cellulose begins to decompose above 220 $^{\circ}$ C when the β -(1-4) glycosidic bonds that form its polymeric structure start to hydrolyze to monosaccharides, which dissolve in the aqueous phase. The hydrochar undergoes

bulk-devolatilization reactions, which cause progressive carbonization (Figure 1 and Table S1) and an improvement in the hydrochar thermal stability (Figure 2). At the same time, furanic compounds in the liquid partially repolymerize into secondary char, while carboxylic acids rearrange and degrade. Residence times have significant effects on the hydrochars and liquid phase compositions, mainly over the HTC range. Among furan compounds, 5-HMF production is maximized at $T < 250\,^{\circ}\text{C}$, which shows the nature of the reaction intermediate by exhibiting a high dependence on reaction time (Figure 5). High temperatures

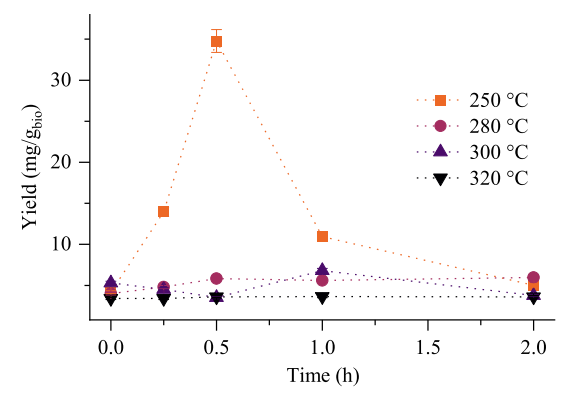


Figure 5. Effects of time on 5-HMF yield from HP of cellulose at different temperatures.

cause rapid repolymerization of 5-HMF to secondary char and rehydration to carboxylic acids, both more stable in the hydrothermal environment due to their polyaromatic nature and the stability of the -COOH group, respectively. Similarly to 5-HMF, reaction time affects the phase properties of other detected compounds more so at low temperatures than when within the HTL regime at the applied heating rates investigated here. Above 250 °C, furans and furfurals give way to cyclopentanone derivatives, which partition into the biocrude. In general, cellulose does not significantly contribute to the formation of biocrude, whose yield remains almost constant with temperature. Indeed, cellulose biocrude has a constant composition characterized by furans at T < 250 °C and, between 250 and 320 °C, by cyclopentanone derivatives with most compounds in the C5-C6 carbon chain range. Despite the enhancement in thermal stability of the hydrochars with the HP severity, some thermally unstable compounds are present over the entire hydrothermal spectrum.

(2) Lignin is more recalcitrant than carbohydrates due to its complex amorphous aromatic polymer structure. It begins to react at low temperatures (even before cellulose) and degrades more significantly above 280 °C, when the VM loss becomes substantial because of increasing carbonization (Table S1). The transition from mild to harsh conditions exhibits several seemingly disparate steps: the first below 200 °C with an initial loss of light volatiles, likely the fragmenting of highly branched heteroatoms from the lignin aromatic core. The second occurs between 220 and 250 °C, corresponding to the first degradation of lignin (mainly

involving hydrolysis). The third happens from 280 to 320 °C, where harsher degradation reactions (like cleavage of ether bonds, C-C bonds, and methoxy groups) cause major structural changes. At reaction temperatures below 280 °C, the hydrochar carbon content slightly improves with temperature as well as its thermal stability, while small amounts of biocrude form. Phenols and methoxyphenols dominate the aqueous phase (Figure 3), and their concentration progressively increases with severity. Lower-molecular-weight carboxylic acids (like lactic, propionic, and acetic acid) are also present. Meanwhile, the biocrude yield increases with the severity of the process, and the biocrude is mainly composed of oxygenated hydrocarbons (mainly phenols and phenol derivatives) in the C6-C9 carbon range. The most abundant compound is guaiacol $(C_7H_8O_2)$, the first degradation product of lignin monomers that then degrades into catechol $(C_6H_6O_2)^{20}$ Residence time slightly impacts the hydrochar and liquid phase compositions.

(3) Willow chips, as a typical lignocellulosic feedstock, exhibit intermediate behavior between cellulose and lignin. Owing to the hemicellulosic fraction, which is characterized by a weaker structure than cellulose and lignin, willow chips start to degrade at lower temperatures in the HTC range. Secondary char derives from both furanic and phenolic compounds. The liquid phase shows the lignocellulosic nature of the feedstock, exhibiting a mixture of furans, carboxylic acids, ketones, and phenols. Furans are predominant at low temperatures, as with pure cellulose, while phenols, deriving from the lignin fraction, increase with severity. Overall, the general behavior is similar to that of cellulose, with an initial decomposition at 220-250 °C, a stabilization at 250-300 °C, and a further decomposition at 300-320 °C.

4. CONCLUSIONS

HPs under subcritical conditions are conventionally distinguished between HTC and HTL. Despite the nomenclature, the transition from mild to harsh conditions (from a reacting system more prone to the production of solid—hydrochar—than liquid—biocrude) is not well defined. This work approached the shift from HTC to HTL by investigating and characterizing the phases from the decomposition of different biomasses (cellulose, lignin, and wood chips). To approach a "real-time" study, we analyzed the solid and liquid phases (aqueous and oily) sampled during the operation. We investigated a wide range of temperatures and residence times (220, 250, 280, 300, and 320 °C at 0, 1/4, 1/2, 1, and 2 h) to provide an insight into the pathways from HTC to HTL.

Results show that the transition from carbonization to liquefaction in terms of reaction temperature and time highly depends on the feedstock composition. Time affects solid and liquid composition in the case of cellulosic feedstock below 250 °C, while temperature is the primary driver at higher temperatures and for lignin. This result indicates that most reactions occur during the heating phase. Longer times are likely to cause slight rearrangements of the phases, which could be helpful to optimize the production of a target product. Cellulosic feedstocks show the first decomposition below 250 °C, characterized by dissolution and repolymerization

reactions. Under these conditions, time is significant and highly affects the formation of intermediates like 5-HMF. Then, only above 300 °C, reactions lead to highly carbonized hydrochar. The cellulose poorly forms biocrude, mainly containing ketones. Hydrochar properties and liquid phase composition more closely resemble those of lignin below 280 °C, mainly due to the aromatic nature of the feedstock. Above that temperature, lignin hydrothermally converts to a more thermally stable hydrochar and phenolic derivatives, which partially repolymerize into the biocrude (mainly consisting of oxygenated hydrocarbons) or secondary char. Time slightly influences the solid and liquid properties of lignin, indicating that most reactions already occur during the adopted heating phase. Wood chips show an intermediate behavior among cellulose and lignin due to their lignocellulosic nature and the hemicellulose fraction.

ASSOCIATED CONTENT

Supporting Information

The Supporting Information is available free of charge at https://pubs.acs.org/doi/10.1021/acssuschemeng.3c07731.

Yields, proximate, and ultimate analyses of all samples; FTIR spectra; and compiled GC-MS results of biocrude from lignin and wood chips (PDF)

AUTHOR INFORMATION

Corresponding Author

Jillian L. Goldfarb — Department of Biological and Environmental Engineering, Cornell University, Ithaca, New York 14853, United States; Smith School of Chemical & Biomolecular Engineering, Cornell University, Ithaca, New York 14853, United States; orcid.org/0000-0001-8682-9714; Email: goldfarb@cornell.edu

Authors

Giulia Ischia — Department of Civil, Environmental and Mechanical Engineering, University of Trento, Trento 38123, Italy; Department of Biological and Environmental Engineering, Cornell University, Ithaca, New York 14853, United States; orcid.org/0000-0001-5878-5603

Hanifrahmawan Sudibyo — Smith School of Chemical & Biomolecular Engineering, Cornell University, Ithaca, New York 14853, United States; orcid.org/0000-0003-1905-129X

Antonio Miotello – Department of Physics, University of Trento, Trento 38123, Italy

Jefferson William Tester – Smith School of Chemical & Biomolecular Engineering, Cornell University, Ithaca, New York 14853, United States

Luca Fiori – Department of Civil, Environmental and Mechanical Engineering, University of Trento, Trento 38123, Italy

Complete contact information is available at: https://pubs.acs.org/10.1021/acssuschemeng.3c07731

Author Contributions

G. Ischia: investigation, methodology, formal analysis, funding acquisition, visualization, and writing—original draft. H. Sudibyo: investigation. A. Miotello: investigation. J.W. tester: supervision, resources, writing—review and editing. L. Fiori: conceptualization, supervision, funding acquisition, writing—review and editing. J.L. Goldfarb: conceptualization, method-

ology, supervision, funding acquisition, resources, writing—review and editing.

Notes

The authors declare no competing financial interest.

ACKNOWLEDGMENTS

Giulia Ischia was financially supported by the U.S.-Italy Fulbright Commission. We thank the financial support provided by the ERICSOL project of the University of Trento. This work was supported by the U.S. National Science Foundation under grants CBET-2031710 and CBET-2144862.

REFERENCES

- (1) Abu-Omar, M. M.; Barta, K.; Beckham, G. T.; Luterbacher, J. S.; Ralph, J.; Rinaldi, R.; Román-Leshkov, Y.; Samec, J. S. M.; Sels, B. F.; Wang, F. Guidelines for Performing Lignin-First Biorefining. *Energy Environ. Sci.* **2021**, *14*, 262–292.
- (2) De Jong, E.; Stichnothe, H.; Bell, G.; Jorgensen, H. Bio-Based Chemicals: A 2020 Update, 2020.
- (3) World Energy Outlook. World Energy Outlook 2021; IEA Publications, 2021; p 15.
- (4) Lozano, E. M.; Pedersen, T. H.; Rosendahl, L. A. Integration of Hydrothermal Liquefaction and Carbon Capture and Storage for the Production of Advanced Liquid Biofuels with Negative CO2 Emissions. *Appl. Energy* **2020**, 279, 115753.
- (5) Nicolae, S. A.; Au, H.; Modugno, P.; Luo, H.; Szego, A. E.; Qiao, M.; Li, L.; Yin, W.; Heeres, H. J.; Berge, N.; Titirici, M. M. Recent Advances in Hydrothermal Carbonisation: From Tailored Carbon Materials and Biochemicals to Applications and Bioenergy. *Green Chem.* **2020**, 22 (15), 4747–4800.
- (6) Castello, D.; Pedersen, T. H.; Rosendahl, L. A. Continuous Hydrothermal Liquefaction of Biomass: A Critical Review. *Energies* (*Basel*) **2018**, *11* (11), 3165.
- (7) Hydrothermal Carbonization and Thermal Hydrolysis—TerraNova®ultra. https://www.terranova-energy.com/en/technology/ (accessed 05 12, 2023).
- (8) (Castellano) Ingelia Technologies—Cleaning the earth to unlock the world Bioeconomy potentials. https://ingelia.com/?lang=en (accessed 05 12, 2023).
- (9) CarboREM—Recovery of Energy and Materials—Greenthesis Group. https://www.greenthesisgroup.com/tecnologie-innovative/carborem-recovery-of-energy-and-materials/ (accessed 05 12, 2023).
- (10) Rizzo, A. M.; Dell'Orco, S.; Miliotti, E.; Chiaramonti, D. Design, Commissioning and Start-up of a New Hydrothermal Liquefaction Continuous Pilot Unit. *Chem. Eng. Trans.* **2020**, *80*, 367–372.
- (11) Castello, D.; Haider, M. S.; Rosendahl, L. A. Catalytic Upgrading of Hydrothermal Liquefaction Biocrudes: Different Challenges for Different Feedstocks. *Renew. Energy* **2019**, *141*, 420–430.
- (12) Ischia, G.; Fiori, L. Hydrothermal Carbonization of Organic Waste and Biomass: A Review on Process, Reactor, and Plant Modeling. *Waste Biomass Valorization* **2021**, *12*, 2797–2824.
- (13) Ischia, G.; Fiori, L. Hydrothermal Carbonization of Organic Waste and Biomass: A Review on Process, Reactor, and Plant Modeling. *Waste Biomass Valorization* **2021**, *12* (6), 2797–2824.
- (14) Tekin, K.; Karagöz, S.; Bektaş, S. A Review of Hydrothermal Biomass Processing. *Renew. Sustain. Energy Rev.* **2014**, 40, 673–687.
- (15) Kruse, A.; Dahmen, N. Hydrothermal Biomass Conversion: Quo Vadis? J. Supercrit. Fluids 2018, 134, 114–123.
- (16) Cao, Y.; He, M.; Dutta, S.; Luo, G.; Zhang, S.; Tsang, D. C. W. Hydrothermal Carbonization and Liquefaction for Sustainable Production of Hydrochar and Aromatics. *Renew. Sustain. Energy Rev.* **2021**, *152* (October), 111722.
- (17) Pecchi, M.; Cascioli, A.; Maag, A. R.; Goldfarb, J. L.; Baratieri, M. Uncovering the Transition between Hydrothermal Carbonization

- and Liquefaction Using Differential Scanning Calorimetry. Fuel Process. Technol. 2022, 235, 107349.
- (18) Kruse, A.; Dahmen, N. Water—A Magic Solvent for Biomass Conversion. *I. Supercrit. Fluids* **2015**. *96*. 36–45.
- (19) Kruse, A.; Dinjus, E. Hot compressed water as reaction medium and reactant. *J. Supercrit. Fluids* **2007**, *39*, 362–380.
- (20) Basar, I. A.; Liu, H.; Carrere, H.; Trably, E.; Eskicioglu, C. A Review on Key Design and Operational Parameters to Optimize and Develop Hydrothermal Liquefaction of Biomass for Biorefinery Applications. *Green Chem.* **2021**, 23 (4), 1404–1446.
- (21) Biller, P.; Riley, R.; Ross, A. B. Catalytic hydrothermal processing of microalgae: Decomposition and upgrading of lipids. *Bioresour. Technol.* **2011**, *102* (7), 4841–4848.
- (22) Zhao, X.; Chen, H.; Kong, F.; Zhang, Y.; Wang, S.; Liu, S.; Lucia, L. A.; Fatehi, P.; Pang, H. Fabrication, Characteristics and Applications of Carbon Materials with Different Morphologies and Porous Structures Produced from Wood Liquefaction: A Review. *Chem. Eng. J.* 2019, 364, 226–243.
- (23) Fan, Y.; Hornung, U.; Dahmen, N.; Kruse, A. Hydrothermal Liquefaction of Protein-Containing Biomass: Study of Model Compounds for Maillard Reactions. *Biomass Convers. Biorefin.* **2018**, 8 (4), 909–923.
- (24) Gallifuoco, A. A New Approach to Kinetic Modeling of Biomass Hydrothermal Carbonization. *ACS Sustain. Chem. Eng.* **2019**, 7 (15), 13073–13080.
- (25) Sandak, A.; Sandak, J.; Waliszewska, B.; Zborowska, M.; Mleczek, M. Selection of Optimal Conversion Path for Willow Biomass Assisted by near Infrared Spectroscopy. *IForest* **2017**, *10* (2), 506–514.
- (26) Besser, K.; Malyon, G. P.; Eborall, W. S.; Paro da Cunha, G.; Filgueiras, J. G.; Dowle, A.; Cruz Garcia, L.; Page, S. J.; Dupree, R.; Kern, M.; Gomez, L. D.; Li, Y.; Elias, L.; Sabbadin, F.; Mohamad, S. E.; Pesante, G.; Steele-King, C.; Ribeiro de Azevedo, E.; Polikarpov, I.; Dupree, P.; Cragg, S. M.; Bruce, N. C.; McQueen-Mason, S. J. Hemocyanin Facilitates Lignocellulose Digestion by Wood-Boring Marine Crustaceans. *Nat. Commun.* **2018**, *9* (1), 5125.
- (27) Wang, H.; Han, X.; Zeng, Y.; Xu, C. C. Development of a Global Kinetic Model Based on Chemical Compositions of Lignocellulosic Biomass for Predicting Product Yields from Hydrothermal Liquefaction. *Renew. Energy* **2023**, *215*, 118956.
- (28) Li, Q.; Liu, D.; Hou, X.; Wu, P.; Song, L.; Yan, Z. Hydro-Liquefaction of Microcrystalline Cellulose, Xylan and Industrial Lignin in Different Supercritical Solvents. *Bioresour. Technol.* **2016**, 219, 281–288.
- (29) Phaiboonsilpa, N.; Champreda, V.; Laosiripojana, N. Comparative Study on Liquefaction Behaviors of Xylan Hemicellulose as Treated by Different Hydrothermal Methods. *Energy Rep.* **2020**, *6*, 714–718.
- (30) Kim, D.; Lee, K.; Park, K. Y. Upgrading the Characteristics of Biochar from Cellulose, Lignin, and Xylan for Solid Biofuel Production from Biomass by Hydrothermal Carbonization. *J. Ind. Eng. Chem.* **2016**, *42*, 95–100.
- (31) Funke, A.; Ziegler, F. Hydrothermal Carbonization of Biomass: A Summary and Discussion of Chemical Mechanisms for Process Engineering. *Biofuels, Bioprod. Biorefin.* **2010**, *4*, 160–177.
- (32) Sharma, H. B.; Sarmah, A. K.; Dubey, B. Hydrothermal Carbonization of Renewable Waste Biomass for Solid Biofuel Production: A Discussion on Process Mechanism, the Influence of Process Parameters, Environmental Performance and Fuel Properties of Hydrochar. Renew. Sustain. Energy Rev. 2020, 123, 109761.
- (33) Volpe, M.; Messineo, A.; Mäkelä, M.; Barr, M. R.; Volpe, R.; Corrado, C.; Fiori, L. Reactivity of Cellulose during Hydrothermal Carbonization of Lignocellulosic Biomass. *Fuel Process. Technol.* **2020**, 206 (February), 106456.
- (34) Falco, C.; Baccile, N.; Titirici, M. M. Morphological and Structural Differences between Glucose, Cellulose and Lignocellulosic Biomass Derived Hydrothermal Carbons. *Green Chem.* **2011**, *13* (11), 3273–3281.

- (35) Kang, S.; Li, X.; Fan, J.; Chang, J. Characterization of Hydrochars Produced by Hydrothermal Carbonization of Lignin, Cellulose, d-Xylose, and Wood Meal. *Ind. Eng. Chem. Res.* **2012**, *51* (26), 9023–9031.
- (36) Liu, J.; Zhang, S.; Jin, C.; Shuang, E.; Sheng, K.; Zhang, X. Effect of Swelling Pretreatment on Properties of Cellulose-Based Hydrochar. *ACS Sustain. Chem. Eng.* **2019**, *7* (12), 10821–10829.
- (37) Ischia, G.; Goldfarb, J. L.; Miotello, A.; Fiori, L. Green Solvents to Enhance Hydrochar Quality and Clarify Effects of Secondary Char. *Bioresour. Technol.* **2023**, 388, 129724.
- (38) Xu, Y. H.; Li, M. F. Hydrothermal Liquefaction of Lignocellulose for Value-Added Products: Mechanism, Parameter and Production Application. *Bioresour. Technol.* **2021**, 342, 126035.
- (39) Cao, L.; Yu, I. K. M.; Liu, Y.; Ruan, X.; Tsang, D. C. W.; Hunt, A. J.; Ok, Y. S.; Song, H.; Zhang, S. Lignin Valorization for the Production of Renewable Chemicals: State-of-the-Art Review and Future Prospects. *Bioresour. Technol.* **2018**, 269 (June), 465–475.
- (40) Mahadevan Subramanya, S.; Savage, P. E. Identifying and Modeling Interactions between Biomass Components during Hydrothermal Liquefaction in Sub-Near-and Supercritical Water. ACS Sustain. Chem. Eng. 2021, 9 (41), 13874–13882.
- (41) Peterson, A. A.; Vogel, F.; Lachance, R. P.; Fröling, M.; Antal Jr, M. J.; Tester, J. W. Thermochemical Biofuel Production in Hydrothermal Media: A Review of Sub- and Supercritical Water Technologies. *Energy Environ. Sci.* **2008**, *1*, 32–65.
- (42) Reza, M. T.; Lynam, J. G.; Uddin, M. H.; Coronella, C. J. Hydrothermal Carbonization: Fate of Inorganics. *Biomass Bioenergy* **2013**, *49*, 86–94.
- (43) Lachos-Perez, D.; Tompsett, G. A.; Guerra, P.; Timko, M. T.; Rostagno, M. A.; Martínez, J.; Forster-Carneiro, T. Sugars and Char Formation on Subcritical Water Hydrolysis of Sugarcane Straw. *Bioresour. Technol.* **2017**, 243, 1069–1077.
- (44) Beckendorff, A.; Lamp, A.; Kaltschmitt, M. Optimization of Hydrolysis Conditions for Xylans and Straw Hydrolysates by HPLC Analysis. *Biomass Convers. Biorefin.* **2023**, *13*, 3361–3374.
- (45) Rissanen, J. V.; Lagerquist, L.; Hemming, J.; Eränen, K.; Eklund, P.; Grénman, H. Intensification of Hydrothermal Biomass Fractionation with the Help of Oxygen: Kinetics and Modeling. ACS Sustain. Chem. Eng. 2022, 10 (38), 12808–12816.
- (46) Reza, M. T.; Rottler, E.; Herklotz, L.; Wirth, B. Hydrothermal Carbonization (HTC) of Wheat Straw: Influence of Feedwater PH Prepared by Acetic Acid and Potassium Hydroxide. *Bioresour. Technol.* **2015**, *182*, 336–344.
- (47) Tsilomelekis, G.; Orella, M. J.; Lin, Z.; Cheng, Z.; Zheng, W.; Nikolakis, V.; Vlachos, D. G. Molecular Structure, Morphology and Growth Mechanisms and Rates of 5-Hydroxymethyl Furfural (HMF) Derived Humins. *Green Chem.* **2016**, *18* (7), 1983–1993.
- (48) Modugno, P.; Titirici, M. M. Influence of Reaction Conditions on Hydrothermal Carbonization of Fructose. *ChemSusChem* **2021**, *14* (23), 5271–5282.
- (49) Yu, S.; Xie, M.; Li, Q.; Zhang, Y.; Zhou, H. Evolution of Kraft Lignin during Hydrothermal Treatment under Different Reaction Conditions. *J. Energy Inst.* **2022**, *103*, 147–153.
- (50) Becker, R.; Dorgerloh, U.; Paulke, E.; Mumme, J.; Nehls, I. Hydrothermal Carbonization of Biomass: Major Organic Components of the Aqueous Phase. *Chem. Eng. Technol.* **2014**, *37* (3), 511–518
- (51) Tkachenko, V.; Marzban, N.; Vogl, S.; Filonenko, S.; Antonietti, M. Chemical Insights into the Base-Tuned Hydrothermal Treatment of Side Stream Biomasses. *Sustain. Energy Fuels* **2023**, 7 (3), 769–777.
- (52) Wüst, D.; Correa, C. R.; Jung, D.; Zimmermann, M.; Kruse, A.; Fiori, L. Understanding the Influence of Biomass Particle Size and Reaction Medium on the Formation Pathways of Hydrochar. *Biomass Convers. Biorefin.* **2020**, *10*, 1357–1380.
- (53) Pedersen, T. H.; Jensen, C. U.; Sandström, L.; Rosendahl, L. A. Full Characterization of Compounds Obtained from Fractional Distillation and Upgrading of a HTL Biocrude. *Appl. Energy* **2017**, 202, 408–419.

- (54) Baccile, N.; Laurent, G.; Babonneau, F.; Fayon, F.; Titirici, M. M.; Antonietti, M. Structural Characterization of Hydrothermal Carbon Spheres by Advanced Solid-State MAS 13C NMR Investigations. *J. Phys. Chem. C* 2009, *113* (22), 9644–9654.
- (55) Qi, Y.; Song, B.; Qi, Y. The Roles of Formic Acid and Levulinic Acid on the Formation and Growth of Carbonaceous Spheres by Hydrothermal Carbonization. *RSC Adv.* **2016**, *6* (104), 102428–102435.
- (56) Qi, Y.; Zhang, M.; Qi, L.; Qi, Y. Mechanism for the Formation and Growth of Carbonaceous Spheres from Sucrose by Hydrothermal Carbonization. *RSC Adv.* **2016**, *6* (25), 20814–20823.
- (57) He, M.; Zhu, X.; Dutta, S.; Khanal, S. K.; Lee, K. T.; Masek, O.; Tsang, D. C. W. Catalytic Co-Hydrothermal Carbonization of Food Waste Digestate and Yard Waste for Energy Application and Nutrient Recovery. *Bioresour. Technol.* **2022**, *344* (PB), 126395.
- (58) Gagić, T.; Perva-Uzunalić, A.; Knez, Z. v.; Škerget, M. Hydrothermal Degradation of Cellulose at Temperature from 200 to 300 °C. *Ind. Eng. Chem. Res.* **2018**, *57* (18), 6576–6584.
- (59) Kruse, A.; Maniam, P.; Spieler, F. Influence of Proteins on the Hydrothermal Gasification and Liquefaction of Biomass. 2. Model Compounds. *Ind. Eng. Chem. Res.* **2007**, 46 (1), 87–96.
- (60) Toor, S. S.; Rosendahl, L.; Rudolf, A. Hydrothermal Liquefaction of Biomass: A Review of Subcritical Water Technologies. *Energy* **2011**, *36*, 2328–2342.
- (61) Yang, J.; He, Q. S.; Niu, H.; Corscadden, K.; Astatkie, T. Hydrothermal Liquefaction of Biomass Model Components for Product Yield Prediction and Reaction Pathways Exploration. *Appl. Energy* **2018**, 228 (April), 1618–1628.
- (62) Liu, H.-M.; Wang, F.-Y.; Liu, Y.-L. Alkaline Pretreatment and Hydrothermal Liquefaction of Cypress for High Yield Bio-Oil Production. *J. Anal. Appl. Pyrolysis* **2014**, *108*, 136–142.
- (63) Sintamarean, I. M.; Grigoras, I. F.; Jensen, C. U.; Toor, S. S.; Pedersen, T. H.; Rosendahl, L. A. Two-Stage Alkaline Hydrothermal Liquefaction of Wood to Biocrude in a Continuous Bench-Scale System. *Biomass Conv. Bioref.* **2017**, *7*, 425.
- (64) González Martínez, M.; Dupont, C.; Thiéry, S.; Meyer, X. M.; Gourdon, C. Impact of Biomass Diversity on Torrefaction: Study of Solid Conversion and Volatile Species Formation through an Innovative TGA-GC/MS Apparatus. *Biomass Bioenergy* **2018**, *119*, 43–53.
- (65) Pedersen, T. H.; Rosendahl, L. A. Production of Fuel Range Oxygenates by Supercritical Hydrothermal Liquefaction of Lignocellulosic Model Systems. *Biomass Bioenergy* **2015**, *83*, 206–215.
- (66) Yong, T. L. K.; Yukihiko, M. Kinetic Analysis of Guaiacol Conversion in Sub- and Supercritical Water. *Ind. Eng. Chem. Res.* **2013**, 52 (26), 9048–9059.
- (67) Wahyudiono; Sasaki, M.; Goto, M. Thermal Decomposition of Guaiacol in Sub- and Supercritical Water and Its Kinetic Analysis. *J. Mater. Cycles Waste Manag.* **2011**, *13* (1), 68–79.
- (68) Wahyudiono; Sasaki, M.; Goto, M. Recovery of Phenolic Compounds through the Decomposition of Lignin in near and Supercritical Water. *Chem. Eng. Process. Process Intensification* **2008**, 47 (9–10), 1609–1619.
- (69) Forchheim, D.; Hornung, U.; Kruse, A.; Sutter, T. Kinetic Modelling of Hydrothermal Lignin Depolymerisation. *Waste Biomass Valorization* **2014**, *5* (6), 985–994.
- (70) Nitsos, C. K.; Choli-Papadopoulou, T.; Matis, K. A.; Triantafyllidis, K. S. Optimization of Hydrothermal Pretreatment of Hardwood and Softwood Lignocellulosic Residues for Selective Hemicellulose Recovery and Improved Cellulose Enzymatic Hydrolysis. ACS Sustain. Chem. Eng. 2016, 4 (9), 4529–4544.
- (71) Chang, C.; Gupta, P. Valorization of Lignin to Obtain Platform Chemicals via Bio-Electrochemical Systems: Batch and Fed-Batch Mode Analysis. *J. Chem. Technol. Biotechnol.* **2023**, *98* (5), 1312–1320.
- (72) Feng, P.; Wang, H.; Lin, H.; Zheng, Y. Selective Production of Guaiacol from Black Liquor: Effect of Solvents. *Carbon Resour. Convers.* **2019**, 2 (1), 1–12.